Thermal characterization of crystalline rocks for cavern thermal energy storage application

Introduction

In Finland, thermal energy storage is gaining increasing commercial interest as district heating sector produces still 72 gCO_2/kWh of emissions in Finland (Energiateollisuus ry, 2025). Thermal energy storage offers a viable solution to still reduce CO_2-emissions by improving energy efficiency and storing waste heat for later use (Reuss, 2015; Sun et al., 2023; Xu et al., 2014). To support these goals, one of the world's largest high-temperature cavern thermal energy storage (CTES) facilities— designed for maximum temperature of 140 °C and storage capacity of 90 GWh—is currently under research and excavation in the city of Vantaa (Vantaa Energia, 2025). As part of the research framework, geological characterization of surrounding rock mass is studied to understand heat losses and ensure efficient operation of the caverns.

The structural and thermophysical properties of rock mass can play a significant role in determining heat losses from CTES systems. One of the most significant risks to thermal efficiency arises from porous layers with groundwater flow (Reuss, 2015). In hard crystalline bedrock environments, such as in Finland, those porous layers are typically associated with fracture or fault zones that can facilitate groundwater movement (Bischoff et al., 2024), which may pose risks to underground thermal energy storage systems (Nilsson and Rohdin, 2019). In addition to groundwater flow, the thermal properties of the rock mass itself can be unfavourable for CTES. Thermal diffusivity is particularly important, as it governs the rate at which heat spreads through the rock mass. Higher thermal diffusivity allows material to react faster to thermal changes (Bergman et al., 2011), potentially increasing heat losses from the storage system. In crystalline rocks, thermal diffusivity is primarily influenced by two factors: thermal conductivity and specific heat capacity (Cermak and Rybach, 1982). A combination of low thermal conductivity and high specific heat capacity is favourable as it minimizes the rate at which heat travels through the rock – an effect described by the thermal diffusivity equation. Lastly, rock density tends to vary within narrow range in crystalline rocks (Waples and Waples, 2004); therefore, it has a relatively minor impact on thermal diffusivity.

This paper presents a comprehensive thermal characterization of the surrounding rock mass at a CTES facility in Vantaa. It combines laboratory and in-situ measurements to evaluate key thermophysical properties and to identify fracture zones associated with groundwater flow. The objective is to enhance understanding of heterogenous subsurface conditions that may affect the performance and thermal efficiency of CTES systems. The results will be used to support future thermophysical modelling.

Methods

As part of a comprehensive sampling campaign, a total of 189 samples were collected from 19 drill cores obtained from the CTES site in Vantaa (Fig. 1). The drill holes were originally drilled for geological characterization purposes, during which three main rock types were identified: granite (97 samples), migmatite (57 samples) and hydrothermally altered rock, helsinkite (22 samples).

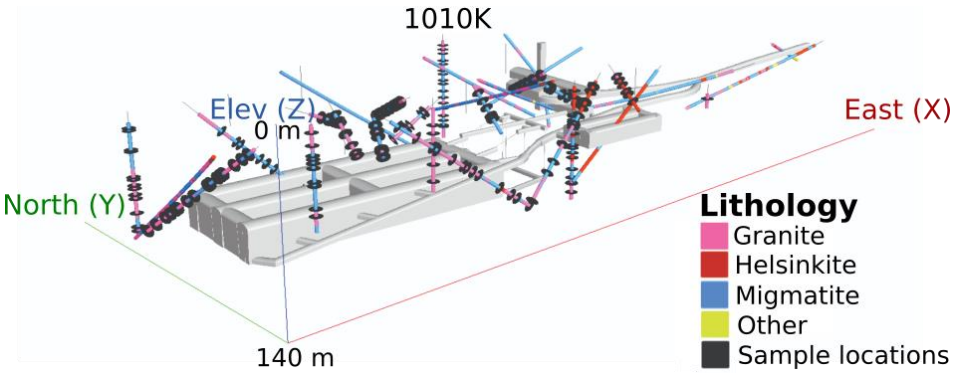

Figure 1. Sample locations at the 1 000 000 m³ CTES site in Vantaa, including also caverns at depth of 100 m; drill holes and observed lithologies based on core data. Drill hole 1010K is named, as its results are presented in the ADTS section.

Of the collected samples, 182 were analysed for thermophysical properties, including thermal conductivity, volumetric heat capacity, density, thermal diffusivity and porosity in the geophysical laboratory of Geological Survey of Finland. Thermal conductivity, volumetric heat capacity, and thermal diffusivity were measured using a Hot Disk TPS 2200 instrument, which is based on the Transient Plane Source (TPS) -method. Prior to measurements, all samples were oven-dried at 105 °C for three days to remove moisture. Each sample was measured twice, and the average of the two was taken as the final result. Density was determined using the Archimedes principle. Each sample was first weighed in air and then weighted in water at a known temperature. The difference in weight was used to calculate the volume displaced, and thus the density. The accuracy of the weighing scale was 0.01 g, with a repeatability better than 0.01%. Finally, specific heat capacity was calculated by dividing volumetric heat capacity by density.

One 140-meter-deep drill hole was measured using the Active Distributed Temperature Sensing (ADTS) method to evaluate effective thermal conductivity of the bedrock and identify fracture zones with groundwater flow. In addition, the ADTS results were compared with laboratory measurements of ten rock samples taken from the corresponding drill core. A fiber optic cable and four heating cables were installed along the entire length of the drill hole. The heating phase lasted 92 hours, during which the drill hole was heated at an average power of 36.4 W m^{-1} using the heating cables. Following the heating period, temperature recovery was monitored for 47 hours. Temperature changes were recorded using a Silixa XT-DTS interrogator, which logged temperature data every two minutes and at 50 cm intervals along the drill hole. These temperature profiles were analysed using the analytical Infinite Line Source (ILS) -method to estimate effective thermal conductivity at 0.5-meter resolution. The groundwater level in this drill hole was at depth of 19 meters. Data above this level were excluded from analysis due to air filled conditions, which introduced convective heat transfer and reduced measurement reliability.

Results

Fig. 2 illustrates the highly heterogenous nature of the three main rock types found at the CTES site. Although the normal distributions and mean values of the most thermal properties appear relatively similar across the rock types (Table 1). However, granite shows a notably narrower range as well as lower values of density.

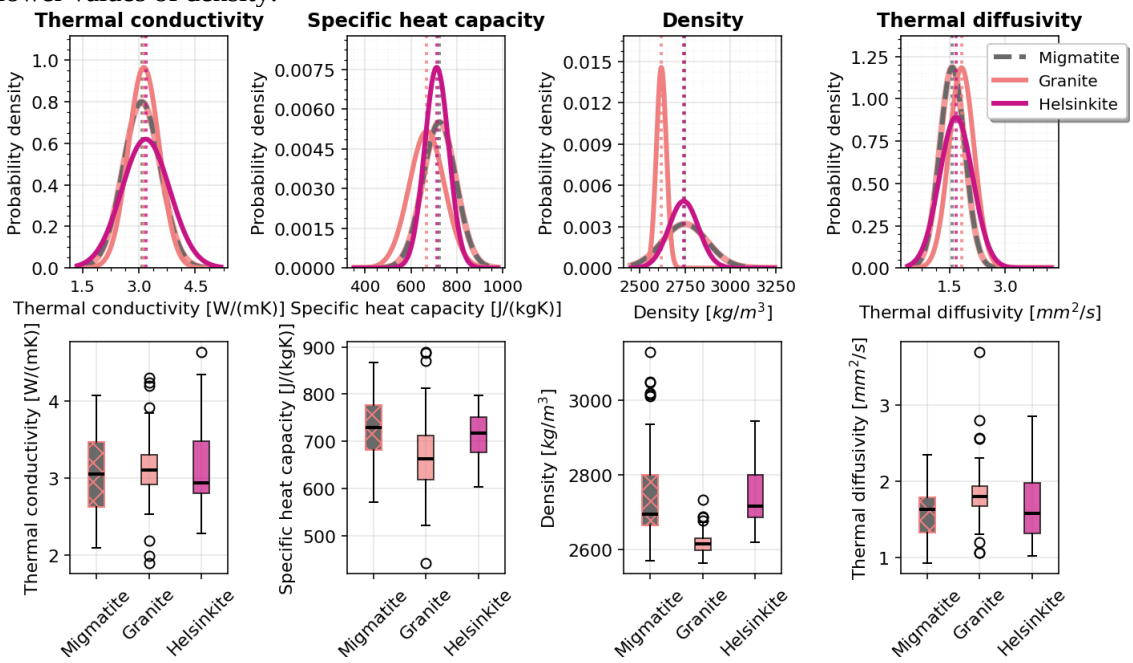

Figure 2. Variation of thermal properties of migmatite, granite and helsinkite at the CTES site. The upper figures show normal distribution of various thermal properties, illustrating significant variability among the rock types. The lower figures display box plots that emphasize the interquartile range (middle 50 %) of the measured values, providing insight into the central tendency, median and variability of the sample results.

Table 1. Average values and standard deviation (σ) of thermal conductivity (k), specific heat capacity (c_p), density (ρ) and thermal diffusivity (α) for identified rocks.

Rock type	k [W/(mK)]		cp [J/(kgK)]		ρ [kg/m³]		α [mm²/s]	
	avg	σ	avg	σ	avg	σ	avg	σ
Granite	3.13	0.50	669	72	2620	30	1.82	0.34
Migmatite	3.07	0.41	725	77	2750	125	1.57	0.34
Helsinkite	3.18	0.64	713	53	2740	80	1.67	0.45

When examining the interquartile ranges (the middle 50 % of the data), migmatite, so called mixed rock, and the hydrothermally altered rock helsinkite show significantly greater variability, indicating higher uncertainty in their thermal properties. Granite, in contrast, shows a narrower spread on thermal conductivity and diffusivity with less uncertainty. In addition, it shows lower values for both specific heat capacity and density. Migmatite and helsinkite display similar ranges and variability in most properties. However, helsinkite shows a distinctly broader spread in thermal diffusivity, indicating greater uncertainty in its thermal response. From an insulation perspective, migmatite statistically offers more favourable thermal properties for CTES at this site. Granite, on the other hand, may exhibit a slightly higher tendency for heat losses due to its higher thermal diffusivity and lower heat capacity.

Since laboratory measurements cannot fully replicate natural groundwater flow conditions, ADTS measurements can offer valuable indications of groundwater movement, as demonstrated in fracture zones FZ4b and FZ5c, where high effective thermal conductivities of 6–7 $W \cdot m^{-1} \cdot K^{-1}$ were observed (Fig. 3). Additionally, lithological variations can be found, for example, at a depth of 40 meters, a lower thermal conductivity of 2.8 $W \cdot m^{-1} \cdot K^{-1}$ coincides with a transition to biotite-rich rock. Furthermore, the heating period generally yields higher effective thermal conductivities compared to the recovery period.

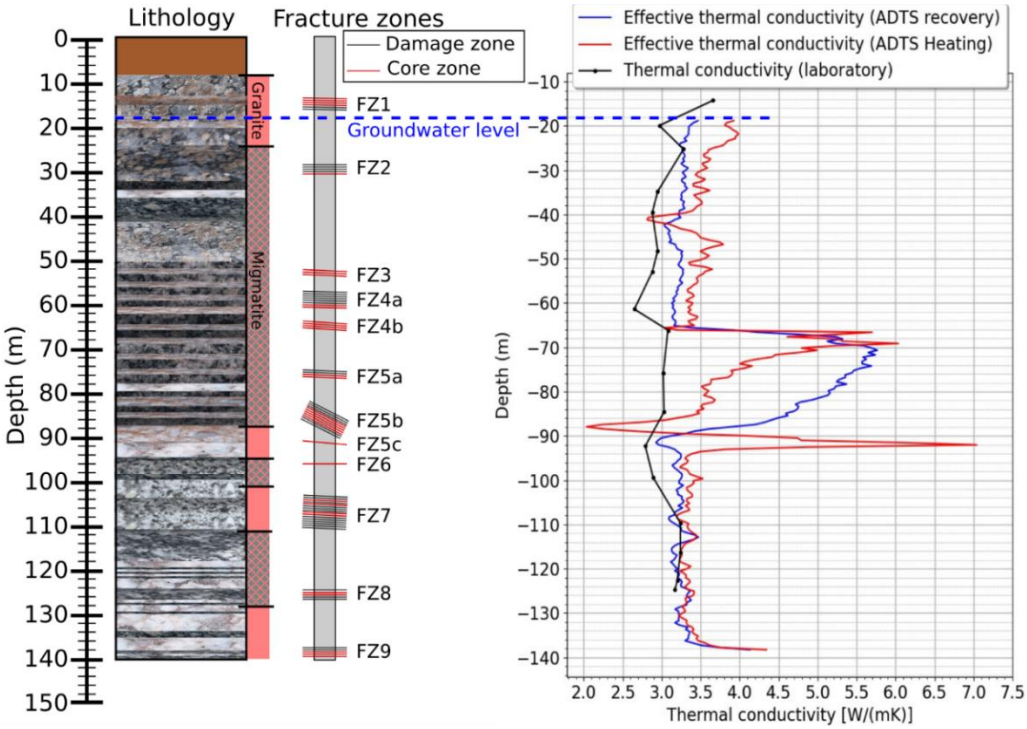

Figure 3. Schematic geological profile of the heterogeneous rock mass at the 1010K drill core, along with a simplified geological interpretation. The figure also includes identified fracture zones and, on the right-hand side, results from ADTS measurements—both heating and recovery phases—showing effective thermal conductivity. Additionally, laboratory-measured thermal conductivity values of rock samples are presented for comparison.

In the upper part of the core, there is a notable difference—approximately 0.25-0.5 $W \cdot m^{-1} \cdot K^{-1}$ between effective thermal conductivity (ADTS; blue/red line) and laboratory-measured values (black line). This discrepancy may indicate the presence of natural convection or groundwater flow within fractures. A particularly large difference in effective thermal conductivity is observed between fracture zones 4b (at 65 m depth) and 5c (at 93 m depth), suggesting active groundwater flow between these zones. This may

imply a hydraulic connection between fractures 4b and 5b. For instance, the mean effective thermal conductivity in situ (3.46 $W \cdot m^{-1} \cdot K^{-1}$) is higher than the average thermal conductivity of dry rock samples measured in the laboratory (3.12 $W \cdot m^{-1} \cdot K^{-1}$), highlighting the influence of groundwater flow on in situ thermal behaviour. Overall, lithological variations appear relatively minor, while the most significant changes in effective thermal conductivity are linked to with fracture zones—supporting the interpretation that groundwater flow influences the thermal behaviour of the bedrock near the CTES.

Conclusions

The results indicate that crystalline rocks at the CTES site in Vantaa exhibit significant heterogeneity. This variability in bedrock introduces uncertainty that must be carefully considered in future thermo-physical modelling aimed at estimating heat losses. In addition, ADTS measurements provide valuable insights into whether subsurface has groundwater flow. Notably, discrepancies between effective thermal conductivity (from in-situ measurement) and laboratory-measured thermal conductivity suggest that fluid movement within fractured zones influences thermal behaviour. Future work will focus on estimating Darcy velocity within these zones and incorporating into thermal models. This will help assess the extent to which groundwater flow affects thermal efficiency and system performance of CTES. Ultimately, accurate modelling of heat losses is essential for the overall energy system design and operation of CTES. Therefore, detailed subsurface characterization—including both thermal and hydraulic properties—is critical for reliable and efficient prediction of CTES system.

Acknowledgements

The present study is financially supported by the EU Horizon Europe project INTERSTORES (project no. 101136100).

References

Bergman, T.L., Incropera, F.P., DeWitt, D.P., Lavine, A.S., 2011. Fundamentals of Heat and Mass Transfer. John Wiley & Sons.

Bischoff, A., Heap, M.J., Mikkola, P., Kuva, J., Reuschlé, T., Jolis, E.M., Engström, J., Reijonen, H., Leskelä, T., 2024. Hydrothermally altered shear zones: A new reservoir play for the expansion of deep geothermal exploration in crystalline settings. Geothermics 118, 102895.

Cermak, V., Rybach, L., 1982. Thermal properties: thermal conductivity and specific heat of minerals and rocks, in: Angeneister, G. (Ed.), Landolt-Bornstein Zahlenwerte and Funktionen Aus Naturwissenschaften Und Technik, Neue Serie, Physichalische Eigenschaften Der Gesteine. Springer-Verlag, Berlin, Heidelberg, New York, pp. 305–343.

Energiateollisuus ry, 2025. Energiavuosi 2024 Kaukolämpö.

Nilsson, E., Rohdin, P., 2019. Performance evaluation of an industrial borehole thermal energy storage (BTES) project – Experiences from the first seven years of operation. Renewable Energy 143, 1022–1034.

Reuss, M., 2015. The use of borehole thermal energy storage (BTES) systems, in: Cabeza, L.F. (Ed.), Advances in Thermal Energy Storage Systems: Methods and Applications. Woodhead Publishing Series in Energy, pp. 117–147.

Sun, M., Liu, Tianze, Wang, X., Liu, Tong, Li, M., Chen, G., Jiang, D., 2023. Roles of thermal energy storage technology for carbon neutrality. Carb Neutrality 2, 12.

Vantaa Energia, 2025. The World's Largest Cavern Thermal Energy Storage [WWW Document]. https://www.vantaanenergia.fi/en/about-us/projects/varanto-the-cavern-thermal-energy-storage/. URL (accessed 6.11.25).

Waples, D.W., Waples, J.S., 2004. A review and evaluation of specific heat capacities of rocks, minerals, and subsurface fluids. Part 1: minerals and nonporous rocks. Natural Resources Research 13, 97–122.

Xu, J., Wang, R.Z., Li, Y., 2014. A review of available technologies for seasonal thermal energy storage. Solar Energy 103, 610–638. https://doi.org/10.1016/j.solener.2013.06.006